Journal of Power Sources 193 (2009) 308–314

Contents lists available at ScienceDirect

Journal of Power Sources

journal homepage: www.elsevier.com/locate/jpowsour

Spatially resolved current density measurements and real-time modelling as a tool for the determination of local operating conditions in polymer electrolyte fuel cells

T. Knöri *, M. Schulze

Institut für Technische Thermodynamik, Deutsches Zentrum für Luft- und Raumfahrt e.V. (DLR), Pfaffenwaldring 38-40, D-70569 Stuttgart, Germany

ARTICLE INFO

Article history:
Received 9 October 2008
Received in revised form 1 December 2008
Accepted 2 December 2008
Available online 25 December 2008

Keywords:
PEFC
Current density distribution
On-line modelling
Cathode
Flow field

ABSTRACT

In this contribution a simplified, isothermal, two-phase, one-dimensional model for the calculation of the cathodic gas flow along the flow field channels of a polymer electrolyte fuel cell (PEFC) is presented. The composition of the humidified oxidant gas, average gas velocity, pressure drop, and other quantities can be calculated for any gas distributor structures with one channel. Thereby, the model requires several input parameters which have to be determined solely by experiment and pre-defined operation conditions, e.g. the water content of the feed gas, local current densities, and gas flow rates. In contrast to other models, the cross-section reduction has been taken into account which results from the penetration of the gas diffusion layer into the flow field channels due to the mounting pressure. Beyond this, the model needs no fit-parameters for further adjustment.

For close examination of the factors limiting the performance of a PEFC, the DLR has developed several techniques for measuring the current density distribution with spatial resolution. In order to investigate the origin of the corresponding effects, one of these techniques has been improved by implementing the model of the cathodic gas flow as an on-line feature.

The combination of a spatially resolved measurement technique with a real-time simulation gives a better understanding of the local processes within the cell and represents a helpful tool for the development of fuel cell components as well as for the optimization of the operating conditions. Exemplarily, the presentation the results for a 25 cm^2 serpentine flow field at different operation modes are shown in this paper.

1. Introduction

Polymer electrolyte fuel cells (PEFCs) are one of the most interesting alternatives for a pollution-free energy production in the fields of portable, mobile, and stationary applications where a highly reliable source of electricity is needed.

One of the major challenges in the development of these powerful devices is to exploit the whole potential of a given membrane electrode assembly (MEA) by an optimized supply of the reaction zone with the reactant gases and an adequate removal of the reaction products. For this purpose, the gas distribution structures, which consist of the gas diffusion layer (GDL) and the flow field have to be optimized.

In combination with an adequate GDL a suchlike improved flow field will provide an optimal distribution of the reactant gases over the entire area of the MEA (and the collection of the exhaust gases, respectively). In addition, it ensures a sufficient humidification of the proton exchange membrane, whereby excess water has to be removed from the cell in order to avoid flooding of the electrodes. Thereby, the water balance is mainly determined by the hydrophobic/hydrophilic character of the GDL.

In practice, not all demands on a gas distributor structure can be fulfilled at the same time, because some of them are inconsistent with one another. For example, the transport of the reactant gases is enhanced by a high porosity of the gas diffusion medium whereas the electrical as well as thermal conductivity suffers from this feature. Hence, local mass transfer and temperature effects still remain obstacles during operation. These phenomena lead to inhomogeneous current distributions resulting in a reduced efficiency of the PEFC.

For a goal-oriented development of gas distributors a deeper insight into the different fuel cell processes in general and the mass transfer in the flow field channels in particular is required. Therefore, the simulation of the gas flow represents an extremely helpful tool. But for reaching a satisfying result, these simulations typically use a huge variety of parameters which can frequently not be related to experimental measurement data, e.g. effective

* Corresponding author. Tel.: +49 711 6862 724; fax: +49 711 6862 322.
E-mail address: torsten.knoeri@dlr.de (T. Knöri).

0378-7753/$ – see front matter © 2009 Elsevier B.V. All rights reserved.
doi:10.1016/j.jpowsour.2008.12.058

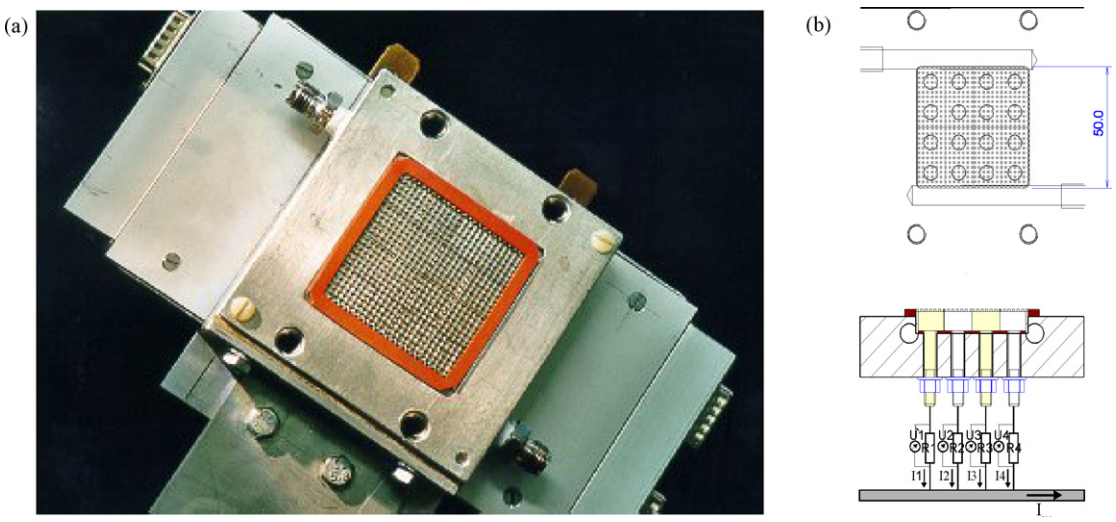

Fig. 1. Anodic flow field with 16 current collector segments for local current density distribution measurement.

transport coefficients. Hence, an approach not relying on fitting parameters has significant advantages for the uniqueness of the results. Furthermore, the mathematical expenditure is extremely high. Consequently, a simultaneous description of the operating state of a fuel cell is not possible while the cell is working.

In this contribution a simplified, isothermal, two-phase model for the calculation of the cathodic gas flux along the flow path in a PEFC is presented. This model requires only input parameters that are determined solely by experiment and can be combined with spatially resolved measurement techniques. This allows an on-line analysis of an operating fuel cell which is extremely helpful for an optimization of the flow field structure but also for the optimization of the operating conditions.

2. Experimental set-up

In order to investigate the important factors for the fuel cell performance, the DLR has developed several measurement and visualization techniques for polymer electrolyte (and solid oxide fuel cells) to determine the local current density distribution in laboratory cells without disturbing the cell operation [1–7]. Fig. 1 displays the design of the anodic flow field, used in this study, whose 25 cm^2 flow field (and current collector) is divided into 16 segments with an area of 1.54 cm^2 for each segment. The current which is generated in a certain region of the MEA flows through the corresponding segment and a small series resistance. Its voltage drop along the resistance is scanned and the resulting current density distribution is registered. For insulating and sealing reasons the individual segments are separated by a silicon cast.

The anodic flow field currently used in this cell has a chocolate wafer structure. But due to the fast kinetics of the hydrogen oxidation, the design of the gas distributor on the anode has no significant impact on the cell performance and the current density distribution, respectively [2–4,8]. In addition, experiments with a segmented cell, which bases on the printed circuit board technology and which provides a higher spatial resolution, have shown that the influence of the flow field segmentation on the fuel cell performance is negligible [5].

While the so-called segmented cell is used as gas distributor and current collector at the anode, the cathode is not segmented and can have various flow field designs. For the measurements mentioned below a flow field with one single channel and a serpentine structure was used. The width and the depth of the channel were 1.0 mm, whereas the land width amounts to 0.5 mm. Fig. 2 shows an illustration of the used flow field. Therein, the characteristic dimensions as well as the direction of the air feed stream are given.

For all electrochemical experiments MEAs with commercial electrode materials purchased from E-TEK® were used. Both on the anode and on the cathode the electrodes contained a Pt-loading of 0.4 mg cm^{-2} with 20 wt.%. Pt/C and single sided backings as gas diffusion layers. In each case the MEAs were prepared by placing the commercial electrodes onto a Nafion®-1135 membrane (purchased from DuPont®) without pressing them together. The final development of a composite structure between the electrodes and the membrane material was achieved by the cell assembling and during an appropriate start-up procedure. The active area of each MEA was 5.0 cm × 5.0 cm.

The assembled cell was fixed in a test set-up which was developed for automatic, continuous, and safety controlled operations

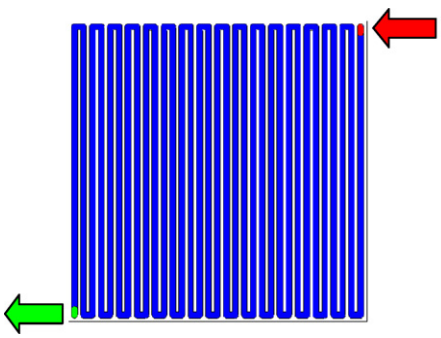

Channel width:	1.0 mm
Channel depth:	1.0 mm
Rib width:	1.0 mm
Total length:	1632 mm
Total area:	25 cm^2

Fig. 2. Scheme of the used serpentine flow field with characteristic dimensions and direction of the air feed stream (cathode).

with hydrogen and air or oxygen. These facilities allow the variation of the operating conditions in a wide range of parameters [9–11]. All experiments were performed with pure hydrogen (type 5.0, Messer Griesheim) and air at pressures of 2.0 bar absolute at the inlet. Both gases were humidified by passing heated bubble columns and kept at the columns' temperature until they reached the fuel cell. For the determination of the water mass flow which is added to the air feed stream, each bubble column was pre-characterized. In this way, the relative humidity of the air stream, φ, can be calculated as a function of the air flux and the water temperature within the bubble column. The cell itself was operated at a temperature of 85 °C.

The electrochemical experiments differed in the adjusted air flow (400, 800, and 2000 sccm) and the corresponding mass flow of water (0.0875, 0.2065, and 0.8132 g min^{-1}). The used hydrogen flow was 240 sccm.

3. Modelling

The main objective of this section is to present the main features of a simple, but unified model that encompasses both the single- and the two-phase regime at the cathode and ensures a smooth transition between the two. In the following, only the basic model assumptions and the main calculation steps for the present problem are summarized. For clarifying the different steps of the modelling procedure, a flow chart is given in Fig. 3.

The used model is strongly simplified in order to reduce the model parameters to a minimum. In this way, the computing time can be reduced, which is necessary for an on-line modelling of the cell operation. The simplifications of the model are listed below:

- The modelling is performed by a one-dimensional model along the cathodic gas channel. Thereby, the thermodynamic state of the corresponding feed stream along the channel is calculated successively by means of experimentally measured data (current density measurements, state of the feed gas at the inlet of the cell) and a simplified water transport across the MEA in order to substitute a reaction and a transport model for the MEA.
- For the calculations with a 1-D model the gas channel is discretized in control volumes that are arranged subsequently along the channel. Thereby, j is used as counting parameter which is related to the position of the control volume.
- Local variations on the anode will be not taken into account in this model.
- Within the model the generation of thermal energy by the non-ideal electrochemical reaction as well as the cooling effect by the evaporation of liquid water is neglected. Consequently, the temperature in the entire fuel cell is regarded as constant and a distribution of the temperature does not occur. The simplification of a fixed temperature is reasonable, because the model is used for interpretation of experiments which are carried out by a single test cell with thick metal end plates and an external temperature control.
- The electrochemical reaction is not simulated, but taken into account by the local current density, which results from an experimental determination of the local mass conversion on the cathode. Hence, the model does not need a sophisticated model for the simulation of the electrochemical reaction that includes the local composition of the reaction gases, the transport processes, the local humidification, etc. The use of the experimentally measured current density distributions allows abstaining from non-understood fitting parameters, which is a significant advantage. The local current density distribution is also the base for the water transport (see below).

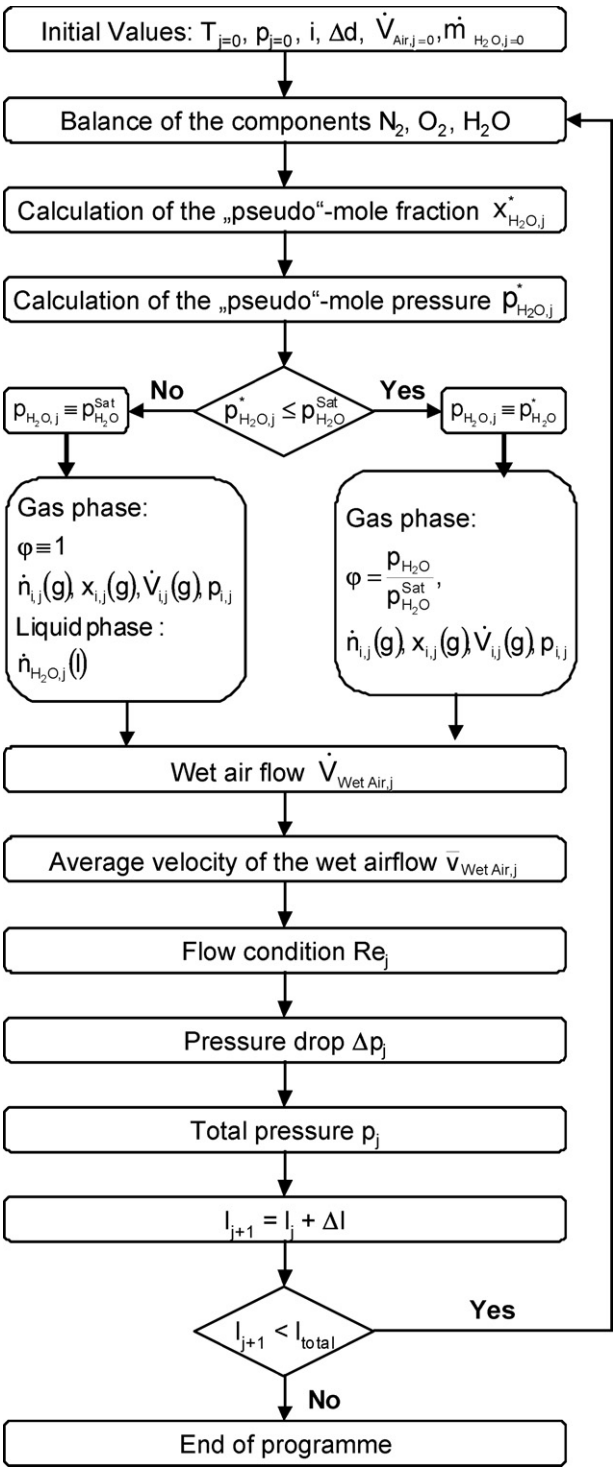

Fig. 3. Flow chart of the modelling routine.

The consumption of oxygen is calculated by means of Faraday's law as a local reaction rate for the control volume j:

$$\dot{n}_{O_2,reac,j} = \frac{A_{MEA,j}}{z_{O_2}\ F}\, i_{MEA,j} \tag{1}$$

Thereby, z_{O_2} represents the number of electrons, which are required for the conversion of one mole oxygen. $i_{MEA,j}$ is the current density in the region of the MEA, $A_{MEA,j}$, that is related to the control volume. As depicted in Fig. 4, the area and the shape of the region $A_{MEA,j}$

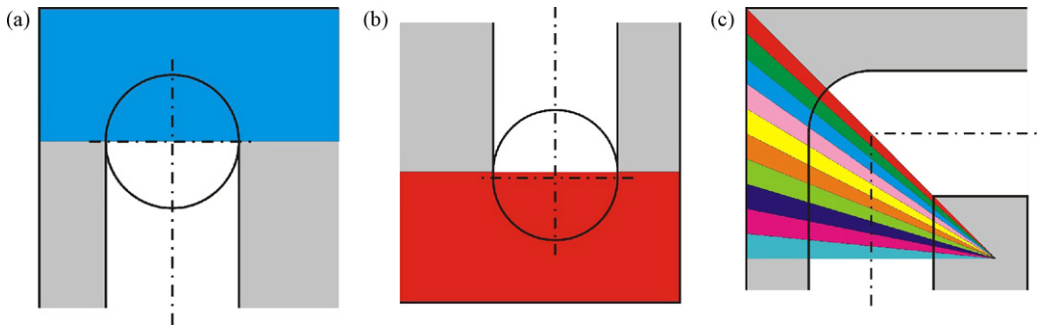

Fig. 4. Partial areas of the MEA, $A_{MEA,j}$, related to a control volume at the: (a) inlet, (b) outlet and (c) at a 90°-bend on the edge of the gas distributor structure.

depends on the position of the corresponding control volume along the channel.

Simultaneously, the consumption of oxygen leads to the formation water. Hence, the water generation rate can be calculated by the equation:

$$\dot{n}_{H_2O,reac,j} = \frac{A_{MEA,j}}{z_{H_2O}\,F} i_{MEA,j} \quad (2)$$

whereby, z_{H_2O} represents the number of electrons, which are necessary for the generation of one mole water.

- The transport processes across the MEA are not simulated. They are reduced to the production of water and the consumption of oxygen at the cathode by the electrochemical reaction as well as to an effective water transport across the membrane. The mass transfer of water through the membrane considers the water drag from the anode to the cathode and the back diffusion in the opposite direction depending on the local current density (0.2 H_2O/H^+ [12,13]). Thereby, the properties of the different membrane-electrode-assemblies and especially the hydrophobic/hydrophilic character of the reaction layer and the gas diffusion layers are neglected.
- Further simplifications refer to the phase state of water. The liquid water phase and the water vapour are resumed to be always in the thermodynamic equilibrium. Therefore, the liquid water phase only exists, if the relative humidity is greater or equal unity (saturation). The relaxation into the state of equilibrium needs no time in the model. In addition, the model supposes that the liquid water phase is transported with the same velocity as the gaseous water vapour phase.

All simplifications concerning the vapour–liquid-equilibrium of water, the mass transfer through the membrane and the velocity of the liquid water along the cathodic gas channel are made with respect to a reduction of the computing time. A more sophisticated model like in Ref. [14] may improve the quality of the simulated results, but it also requires significantly more computing power. Consequently, an extremely detailed modelling cannot be easily implemented into the presented measurement technique and cannot be used as a feature of an on-line tool.

Furthermore, it should be noted that, since the model does not include effects on electrode level, no direct interpretations of electrode processes are possible. However, the local performance of the MEA is an input parameter into the model evaluation that enables an interpretation of the channel state. From this information also plausible deductions on the local operating states of the electrodes can be drawn.

For starting the simulation, the model requires several initial values. These parameters include the thermodynamic state of the cathodic feed gas at the inlet, which is experimentally determined as well as values which are given by the experimental set-up. The main parameters for the simulation of the cathodic gas flux are the adjusted air flow, $\dot{V}_{air,j=0}$, the inserted mass flow of water in the air feed stream by the bubble column, $\dot{m}_{H_2O,j=0}$, as well as the operating temperature, $T_{j=0}$, and the pressure at the inlet of the cell, $p_{j=0}$. In addition, the model requires data about the flow field and its conduit, which includes the flow field design and the reduction of the channel's cross-section by impression of the gas diffusion layer into the channel due to the clamping pressure as depicted in Fig. 5 [15]. As described above, for the consideration of the chemical reaction the measured current density distribution, i, was used. Hence, the MEA, the GDL, and the processes within can be regarded as a "black box".

After setting the initial values on the basis of the experimental data in each control volume along the channel, the steps which are described below are performed. Thereby, the outlet values for each element become the inlet values for the following one. In this way, the control volumes are handled subsequently until the outlet of the cell is reached.

Based on this set of parameters, a molar balance for the different components of the humidified air flow is established for the inlet of the fuel cell ($j = 0$). This balance is divided into two steps and considers the oxygen consumption as well as the water generation at the membrane/cathode interface calculated by means of the current density distribution measurements and the corresponding mass conversion. To this point, the distinct state of the water – liquid or gaseous – is neglected.

Therefore, the resulting mole fractions were declared as "pseudo"-mole fractions (x_i^*). By means of the "pseudo"-mole fraction for the water and the total pressure at this position, a "pseudo"-partial pressure ($p_{H_2O}^*$) can be calculated.

This parameter helps to determine, if the water exists as vapour or in a liquid form at this position of the channel. Subsequently, in a second step the "pseudo"-partial pressure is compared with the saturation pressure of water which can be calculated by Antoines's law [16]. If the "pseudo"-partial pressure is less or equal than the saturation pressure the humidified air is not oversaturated and its relative humidity is less or equal to unity. In this case, no liquid

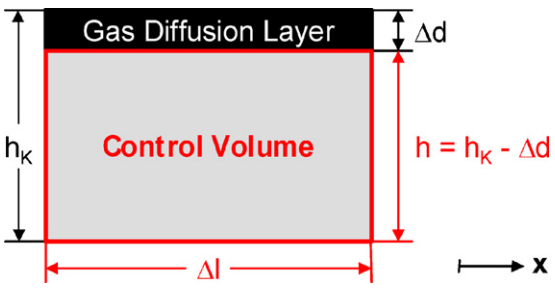

Fig. 5. Differential cross-section of a control volume within the cathodic gas channel (channel width: b; channel height: h; depth of impression of the GDL: Δd).

water phase exists at the entrance of the fuel cell and the "pseudo"-mole fractions for the different components correspond to the real mole fractions as calculated before. In contrast, if the "pseudo"-partial pressure is greater than the value of the saturation pressure the humidified air is oversaturated and a liquid phase appears. In this case, the relative humidity is set to unity and the composition for the gaseous phase has to be calculated anew (x_i, p_i).

With the assumptions that the volume of the liquid phase is negligible and that the velocities of the liquid and the gaseous water phase are equal, the total flux of the wet air and its velocity, respectively, can be calculated for all cases: dry, unsaturated, saturated and oversaturated wet air. According to the channel geometry, the reduction of the duct cross-section by the penetration of the backing material in the gas distributor structure as well as the Chapman–Enskog-equation for the calculation of the viscosity, the flow condition can be determined by the Reynolds number [17].

Depending on the flow condition – laminar or turbulent – the pressure drop, Δp_j, over a differential segment of the channel with the length Δl can be evaluated. Its calculation is based on the general equations for the pressure drop in channels with a rectangular cross-section and for 90°-bending curve [17].

For the determination of the air composition at this position the calculation has to start anew with a molar balance for the different components as it was mentioned above. In this way, a flow field on the cathode side can be calculated step by step from the inlet ($l = 0$) to the outlet ($l = l_{\text{total}}$).

Recapitulating, the model uses as input parameter the cathodic air flux and its water content, the measured current density distribution, and the given flow field geometry for the calculation of local values like the composition of the wet air flow, the partial pressures of all components, the average gas velocity as well as the phase state of water. Moreover, the impression depth of the gas diffusion layer into the flow field channels is considered which can be quantified by several methods [15]. Thereby, the focus of the model is not the prediction of the fuel cell behaviour or the corresponding performance, but the interpretation of fuel cell experiments.

For validating the simulation model, the calculated humidity as well as the total pressure of the cathodic outlet stream were compared with measured values. Thereby, differences in a range of ±10% were observed which are tolerable for the desired application area.

Table 1
Composition of the air feed stream at the cell inlet and current obtained at 500 mV (the values in the table are experimentally determined start values for the calculation of the local gas composition and the pressure along the channel in the cathodic flow field).

No. (–)	Air flow rate (sccm)	Water vapour mass flow (g min^{-1})	Relative humidity (–)	Current [A]
I	400	0.0875	0.68	14.1
II	800	0.2065	0.80	16.9
III	2000	0.8132	1.00	18.6

In contrast, locally resolved pressure and humidity values along the gas channels cannot be performed presently, because sensors for these quantities have not been implemented into the segmented cell technology yet.

4. Results and discussion

By means of the following three examples the combination of experimental current density distribution measurements and the evaluation of the data with the model described above will be given. These experiments differ in the adjusted air flow rate and the water content. Table 1 gives an overview about the different settings of the oxidant feed stream at the inlet of the fuel cell. The hydrogen flow was kept at 240 sccm in all experiments. In Fig. 6 the current density distributions measured at a cell potential of 500 mV are displayed.

All of the three diagrams show a similar structure of the current density distribution. Starting from the gas inlet in the upper corner on the right the current generation increases along the direction of the gas flow. After passing a global maximum, the current density declines towards the outlet continuously. A closer look on the regions with the highest current densities reveals that a strong dependency between the global maximum, the adjusted air flux, and the humidification conditions exists. The higher the air flow rate and the higher the water vapour flux, respectively, the higher is the current density at the gas inlet as well as the maximum value of the whole current density distribution. Simultaneously, the position of the maximum is moved in the flow direction towards the outlet in accordance with an increase of the air flow rate and the water content of the humidified air.

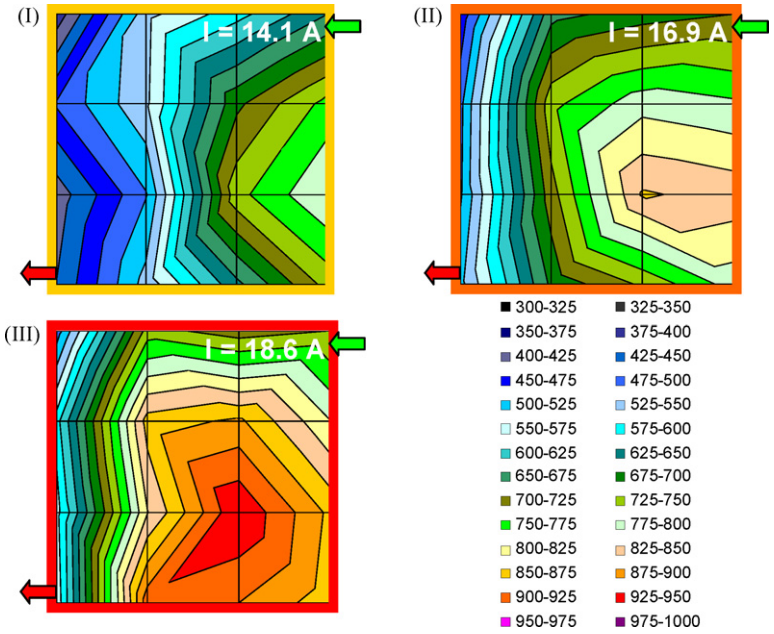

Fig. 6. Measured current density distributions in mA cm^{-2} under different operating conditions (referring to Table 1) at a cell potential of 500 mV [air flow rate: (I) 400 sccm, (II) 800 sccm, and (III) 2000 sccm; the orientation of the flow field corresponds to Fig. 2].

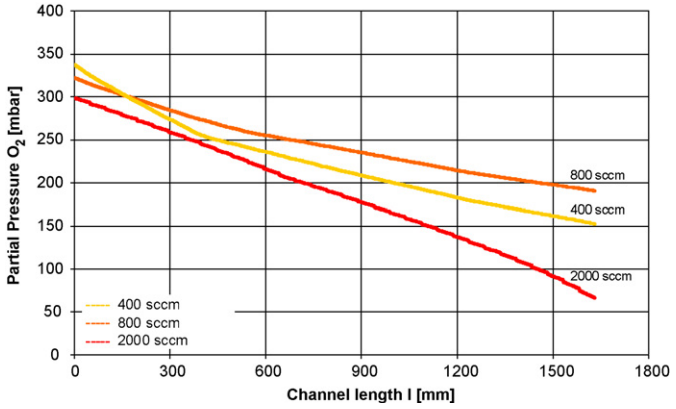

Fig. 7. Calculated partial pressure of oxygen at different air flow rates along the flow field channel of the serpentine gas distributor.

Without further information this behaviour of the fuel cell would be interpreted as identical for each of the three experiments. But in contrast, an evaluation of the experimental data by using the model described above reveals that the situation within the cell may differ completely. For these purposes, the thermodynamic states of the cathodic feed streams along the gas distributor channel were calculated from the experimental data (operating conditions and measured current density distribution). The calculated oxygen pressure along the channel is displayed in Fig. 7, the corresponding relative humidification is shown in Fig. 8 for all of the three air flow rates.

The partial pressure of oxygen typically has a fundamental influence on the rate of the electrochemical reaction and accordingly on the entire consumption of oxygen. Along its way through a gas distributor the partial pressure of oxygen in humidified air suffers from two different mechanisms. On the one hand, the partial pressure is reduced by the chemical conversion at the cathode. At a constant current density this influence grows with reduced air flux. On the other hand, the partial pressure declines proportionally to a reduction of the total pressure. This effect becomes important at higher air flow rates when the pressure drop rises significantly.

A comparison of the partial pressures of oxygen for the different electrochemical experiments demonstrates the impact of each single effect while they are superimposed.

Due to the humidification the cathodic air flux in the bubble columns contains vapourous water, so that the partial pressure of oxygen is lower than 21% of the total pressure at the inlet ($p_{j=0}$ = 2 bar). When the air flow rate is increased from 400 to 800 sccm the reduction of the partial pressure along the channel is less pronounced. However, if the flow rate is increased from

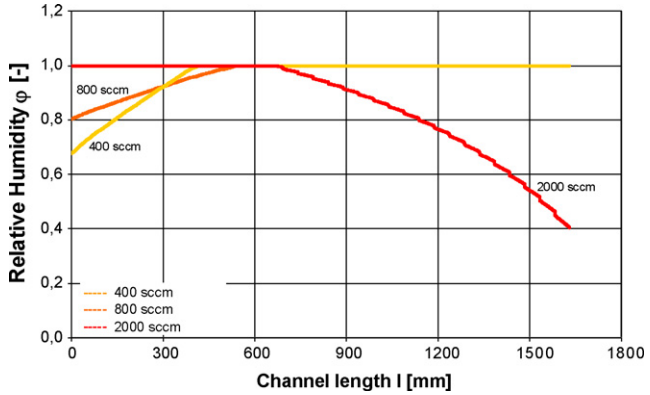

Fig. 8. Calculated relative humidity at different air flow rates along the flow field channel of the serpentine gas distributor.

400 to 2000 sccm, the oxygen partial pressure decreases strongly along the channel. In this regard, it is noted that the dependence of the pressure drop on the flow rate is very distinctive. Whereas a change from 400 to 800 sccm increases the pressure drop from 72.5 up to 162.9 mbar (a factor of approx. 2) the variation from 400 to 2000 sccm results in a pressure drop of around 1 bar (a factor of 15). Due to the increasing mass flow an increase of a factor 5 would be expected, but in addition, the flow type changes from laminar to turbulent, inducing an increase of the flow resistance and consequently an additional significant increase of the pressure drop. For this reason, the effect of an increasing pressure drop with the flow rate has only a low impact on the partial pressure and the pressure drop for the change from 400 to 800 sccm. In contrast, the chemical reaction relatively consumes more oxygen due to the higher current production. But as a result of the doubled air flux the mole fraction of oxygen remains higher. Therefore, the reduction of the partial pressure of oxygen is dominated by the oxygen consumption which leads to a smaller decrease for the higher air flow rate.

When the air flow rate is adjusted to 2000 sccm the importance of both effects is reversed. In this case, the reduction of the partial pressure is mainly determined by the increase of the pressure drop which is nearly 15 times higher than at an air flux of 400 sccm. In contrast, the oxygen consumption that reduces the oxygen fraction of the air stream is only marginal has no significant influence on the partial pressure.

The oxygen partial pressures do not explain the recorded current density distributions. Hence, another parameter must have a more significant influence on the variation of the local electrochemical performance.

It is well known that the humidification has a strong influence on the membrane conductivity and consequently on the electrochemical performance. Therefore, the local water content and the relative humidification, respectively, were calculated with the model. In the first experiment which is performed with an air flux of 400 sccm the air entering the cell is too dry for a complete humidification of the polymer electrolyte. Hence, the proton conductivity becomes the limiting factor for the electrochemical conversion in this region. Along the channel the water generation leads to an increasing relative humidity which improves the conductivity of the membrane and thereby the local electrochemical performance. Directly at the inlet water is only present as vapour. But as a result of the gradually increase of the water generation rate the relative humidity approaches unity. At this point, the water condenses and a two-phase flow is developed. It is noted in this respect that the membrane material (Nafion®) is humidified more effectively from liquid water compared to water vapour. As a consequence of the presence of liquid water the membrane conductivity increases along the channel, but simultaneously the oxygen transport is more and more hindered by the liquid phase. Therefore, the local electrochemical performance decreases after the formation of liquid water. Consequently, the maximum of the current density is positioned near the middle of this region and marks the position where the water flux changes from a single vapour phase to a vapour–liquid system.

A doubling of the air flow keeps the behaviour of the water similar, but the maximum of the current density is shifted in the flow direction to the middle of the cell. Due to the higher flow rate the increase of the humidification along the channel is lower, because the conversion of oxygen to water is not doubled, too. This is related to the changes of the oxygen partial pressure as discussed above.

In contrast to the first two experiments, at the high air flow rate of 2000 sccm the air flux becomes oversaturated with water meaning a liquid water phase already enters the cell. Caused by the higher gas velocity and the resulting high pressure drop over the cell the liquid water evaporates along the channel and the relative humidification decreases. In contrast to the other experiments described

above the liquid water hinders the oxygen transport in the first section of the cell and the drying of the membrane reduces the electrochemical performance towards the end of the channel. As a result of these experiments the maximum current density remains in the middle of the active area, like in other experiments, but the reason for this current density distribution is completely different. The position of the maximum here indicates the complete evaporation of the liquid water phase.

5. Conclusion

The three experiments show clearly that diametrical effects influence the oxygen partial pressure as well as the water content of the air flux. Based on that knowledge, it can be derived that by variation of the air flow rate and its water content the humidification, the oxygen partial pressure as well as the extension of the area with a high local electrochemical performance can be locally adjusted.

For all experiments the measured current density distributions have a similar appearance, whereby the maximum marks the transition from a single to a two phase flow of water and vice versa. The real conditions inside the cell differ significantly between the various experiments, but only by means of the current density distribution measurements the local operating conditions cannot be explained. Consequently, for a distinct evaluation of the experimental data a simple modelling is essential for the understanding of the basic processes and the local operating conditions within a fuel cell.

For this purpose, an isothermal two-phase flow and transport model was developed and combined with the segmented cell technology for the determination of locally resolved current density distributions. The crucial parts of this model are the analysis of the formation of liquid water, its effects on the local cell performance and the composition of the air feed stream on its way along the cathode.

In the present case, the simulation of the cathodic gas flow clearly reveals that the different states within the cell strongly depend on the adjusted operating conditions, even if the measured current density distributions resembles each other.

While one set of operating parameters leads to a successive flooding of the channel structure from the inlet to the outlet, slightly changed operating conditions results in a dry up of the cell.

These conclusions mainly result from the simulation. Hence, the combination of current density measurements and modelling represents an extremely powerful tool for the investigation and the design of flow fields as well as for the on-line analysis of fuel cells and the development of control strategies. Moreover, the real-time simulation of the cathodic gas flow within helps optimizing the operating conditions of the cell.

References

[1] Ch. Wieser, A. Helmbold, E. Gülzow, J. Appl. Electrochem. 30 (2000) 803.
[2] E. Gülzow, S. Schönbauer, Proceedings of the Fuel Cell Seminar, Miami, USA, 475 (2003) 252.
[3] E. Gülzow, T. Kaz, R. Reißner, H. Sander, L. Schilling, M.v. Bradtke, J. Power Sources 105 (2002) 261.
[4] E. Gülzow, Proceedings of the Otti-Seminar: Neuntes Fachforum Brennstoffzellen, Ulm, Germany, 2002, p. 293.
[5] M. Schulze, E. Gülzow, S. Schönbauer, T. Knöri, R. Reissner, J. Power Sources 173 (2007) 19.
[6] P. Metzger, K.-A. Friedrich, H. Müller-Steinhagen, G. Schiller, Solid State Ionics 177 (2006) 2045.
[7] K.A. Friedrich, P. Metzger, G. Schiller, H. Müller-Steinhagen, ECS Transactions 7 (2007) 1841.
[8] N. Wagner, in: E. Barsoukov, J.R. Macdonald (Eds.), Impedance Spectroscopy: Theory, Experiment, and Applications, John Wiley & Sons, New York, 2005.
[9] E. Gülzow, A. Helmbold, T. Kaz, R. Reißner, M. Schulze, N. Wagner, G. Steinhilber, J. Power Sources 86 (2000) 352.
[10] S. Weißhaar, R. Reissner, W. Schröder, E. Gülzow, J. Power Sources 118 (2003) 405.
[11] W. Schröder, D. Bevers, MessTec 6 (1997) 243.
[12] T.A. Zawodzinski, C. Derouin, S. Radzinski, R.J. Sherman, T. Smith, T.E. Springer, J. Electrochem. Soc. 140 (1993) 1041.
[13] T.A. Zawodzinski, T.E. Springer, J. Davey, R. Jestel, C. Lopez, J. Valerio, S. Gottesfeld, J. Electrochem. Soc. 140 (1993) 1981.
[14] X. Xue, J. Tang, J. Fuel Cell Sci. Technol. 2 (2005) 274.
[15] T. Knöri, M. Schulze, E. Gülzow, Proceedings of the 2nd European Fuel Cell Technology and Applications Conference, Rome, Italy, 2007, p. 73.
[16] Verein deutscher Ingenieure—VDI-Gesellschaft Verfahrenstechnik und Chemieingenieurwesen [Eds.], VDI-Wärmeatlas—Berechnungsblätter für den Wärmeübergang, Düsseldorf, 1984.
[17] W. Wagner, Strömung und Druckverlust, Würzburg, 1997.